The Journal of Immunology

RESEARCH ARTICLE | FEBRUARY 01 2007

Effects of Vascular Endothelial Growth Factor on the Lymphocyte-Endothelium Interactions: Identification of Caveolin-1 and Nitric Oxide as Control Points of Endothelial Cell Anergy[1] FREE

Caroline Bouzin; ... et. al

J Immunol (2007) 178 (3): 1505–1511.
https://doi.org/10.4049/jimmunol.178.3.1505

Effects of Vascular Endothelial Growth Factor on the Lymphocyte-Endothelium Interactions: Identification of Caveolin-1 and Nitric Oxide as Control Points of Endothelial Cell Anergy[1]

Caroline Bouzin, Agnès Brouet, Joelle De Vriese, Julie DeWever, and Olivier Feron[2]

Tumors may evade immune responses at multiple levels, including through a defect in the lymphocyte-vessel wall interactions. The angiogenic nature of endothelial cells (EC) lining tumor blood vessels may account for such anergy. In this study, we examined whether mechanisms other than down-regulation of adhesion molecules could be involved, particularly signaling pathways dependent on the caveolae platforms. To mimic the influence of the tumor microenvironment, EC were exposed to TNF-α and the proangiogenic vascular endothelial growth factor (VEGF). We identified a dramatic inhibition of lymphocyte adhesion on activated EC following either short or long VEGF pretreatments. We further documented that VEGF did not influence the abundance of major adhesion molecules, but was associated with a defect in ICAM-1 and VCAM-1 clustering at the EC surface. We also found that overexpression of the caveolar structural protein, caveolin-1, overcame the VEGF-mediated inhibition of adhesion and restored ICAM-1 clustering. Conversely, EC transduction with a caveolin-1 small interfering RNA reduced the TNF-α-dependent increase in adhesion. Finally, we identified VEGF-induced NO production by the endothelial NO synthase as the main target of the changes in caveolin-1 abundance. We found that the NO synthase inhibitor *N*-nitro-L-arginine methyl ester could reverse the inhibitory effects of VEGF on lymphocyte adhesion and EC cytoskeleton rearrangement. Symmetrically, a NO donor was shown to prevent the ICAM clustering-mediated lymphocyte adhesion, thereby recapitulating the effects of VEGF. In conclusion, this study provides new insights on the mechanisms leading to the tumor EC anergy vs immune cells and opens new perspectives for the use of antiangiogenic strategies as adjuvant approaches to cancer immunotherapy. ***The Journal of Immunology,*** **2007, 178: 1505–1511.**

The $CD8^+$ cytolytic T lymphocytes play crucial roles in host defense against tumors (1, 2). Tumor cells may, however, evade immune responses at multiple levels within the effector-target interaction (3). For instance, a deficiency in leukocyte adhesion to the endothelium lining tumor blood vessels is proposed as one possible mechanism of resistance to immunotherapy (4). The tumor microenvironment and, more particularly, the ongoing angiogenesis is very likely to account for the anergy of the tumor vessel endothelium. Several studies have explored the impact of angiogenic growth factors on the adhesion of a variety of immune cells on cultured endothelial cells (EC)[3] (5–9). In most of these studies, a decrease in the expression of adhesion molecules was identified as a major cause of the deficit in immune cell adhesion to neoformed vessels. Such focus on the alterations in the gene expression pattern, determined by key angiogenic cytokines, such as the vascular endothelial growth factor (VEGF) (10), may have led to underestimates of other mechanisms.

Two sets of independent studies suggest that the structural protein of caveolae, caveolin-1, could be critical in regulating the adhesion process at the signaling (vs gene expression) level. First, the role of caveolae in transcellular migration was recently demonstrated in studies identifying the association of caveolin-1 with structures called transmigratory cups (11) or F-actin ring-rich channels (12), which provide directional guidance to leukocytes for extravasation. Second, caveolae are described as signaling platforms concentrating key actors, including the VEGF receptor 2 (13, 14). We recently documented, by comparing the vascular phenotype of wild-type and caveolin-1-deficient mice, the key role of caveolae in regulating the activity of the endothelial NO synthase (eNOS) in a model of VEGF-dependent postischemic angiogenesis (14). In the line of the potential multiple down-regulatory roles of VEGF on lymphocyte adhesion, one may, therefore, ask whether caveolae might also influence the adhesion process in tumor EC through direct caveolin-regulated signaling pathways.

In this study, we aimed at identifying the potential effects of VEGF on lymphocyte adhesion to activated EC, independent of changes in the abundance of adhesion molecules. We also examined whether endogenous caveolin-1 was involved in such effects and whether its molecular up- or down-regulation could influence the process of adhesion on TNF-α-activated EC.

Université Catholique de Louvain Medical School, Unit of Pharmacology and Therapeutics, Brussels, Belgium

Received for publication March 22, 2006. Accepted for publication November 8, 2006.

The costs of publication of this article were defrayed in part by the payment of page charges. This article must therefore be hereby marked *advertisement* in accordance with 18 U.S.C. Section 1734 solely to indicate this fact.

[1] This work was supported by grants from the Fonds de la Recherche Scientifique Medicale, the Fonds National de la Recherche Scientifique, the Televie, the Belgian Federation against Cancer, the J. Maisin Foundation, and Action de Recherche Concertee (ARC 04/09-317) from the Communaute Française de Belgique. O.F. is a Fonds National de la Recherche Scientifique Senior Research Associate.

[2] Address correspondence and reprint requests to Dr. Olivier Feron, Université Catholique de Louvain Medical School, Unit of Pharmacology and Therapeutics, FATH 5349, 52 Avenue E. Mounier, B-1200 Brussels, Belgium. E-mail address: feron@mint.ucl.ac.be

[3] Abbreviations used in this paper: EC, endothelial cell; VEGF, vascular endothelial growth factor; eNOS, endothelial NO synthase; HMVEC, human microvascular EC; NOx, NO derivative; siRNA, small interfering RNA; DETA, diethylenetriamine; L-NAME, *N*-nitro-L-arginine methyl ester; Ct, cycle threshold; NOS, NO synthase.

Materials and Methods

Cell culture

HUVEC and dermal-derived human microvascular EC (HMVEC) were purchased from Cambrex and were routinely cultured on 0.2% gelatin-coated dishes in EGM and EGM-2MV (Cambrex), respectively. Jurkat T cells were obtained from American Type Culture Collection and cultured in 10% serum containing RPMI 1640 medium. In some experiments, HMVEC were transfected with 1 μg of caveolin-1-encoding plasmid (per 6-well dish) (14) or with 5 μg of caveolin-1 small interfering RNA (siRNA; sequence: aagatgtgattgcagaaccag) using Lipofectin reagent (Invitrogen Life Technologies) according to the manufacturer's protocol.

Lymphocyte isolation

Human $CD8^+$ T lymphocytes were prepared from blood buffy coats or from healthy blood donors. Mononuclear cells were isolated by density gradient centrifugation on a Histopaque-1077 gradient according to the manufacturer's protocol (Sigma-Aldrich). The $CD8^+$ cells were isolated by MACS. Isolated $CD8^+$ cells were used immediately after isolation. The purity of the positive fraction was confirmed by flow cytometry and was >90%.

Adhesion assay

EC, grown to confluence on 12-well dishes, were stimulated for 4 h with 40 U/ml TNF-α (R&D Systems) before the addition of $CD8^+$ or Jurkat T cells (10^6/ml). After 60 min of incubation at 37°C, unadhered cells were removed by washing. Before stimulation, cells were treated with VEGF (100 ng/ml; R&D Systems) for a short (30 min) or long (16 h) period. In some experiments, cells were incubated for 1 h with 20 μg/ml blocking Abs directed against ICAM-1 (clone BBI6-I1; R&D Systems), VCAM-1 (clone 1.G11B1; BioSource International), E-selectin (clone BBIG-E4; R&D Systems), or P-selectin (clone 9E1; R&D Systems) before the addition of immune cells. In other experiments, *N*-nitro-L-arginine methyl ester (L-NAME, 5 mM) or diethylenetriamine NO (DETA-NO, 100 μM) were added 30 or 15 min before VEGF treatment, respectively. The number of adherent $CD8^+$ cells was counted in three to four microscopic fields (0.5 mm^2/field).

Flow cytometry

Cells collected by brief exposure to trypsin were incubated for 20 min at 4°C with a fluorescein-conjugated anti-ICAM-1 mAb (clone BBIG-I1, 1/10 dilution; R&D Systems) or FITC-conjugated anti-VCAM-1 mAb (clone 51-10C9, 1/5 dilution; BD Pharmingen). Negative controls were cells incubated without Abs. Labeled cells were fixed in 1.25% paraformaldehyde, and fluorescence intensity was measured using a FACScan apparatus (BD Biosciences) and was analyzed by the CellQuest software (BD Biosciences).

Immunofluorescence microscopy

For ICAM-1 labeling, EC were cultured on gelatin-coated LabTek chambers or coverslips and were stimulated following the same protocol as for the adhesion assays. Cells were fixed with 4% paraformaldehyde/0.1% glutaraldehyde in PBS for 20 min at room temperature. For the visualization of ICAM-1 clustering, fixed cells were incubated with quenching buffer (2% BSA/0.1 M glycine/PBS) at room temperature for 5 min and then in blocking buffer (2% BSA/PBS) at 37°C for 30 min. Incubation with a mouse monoclonal anti-human ICAM-1 Ab (1/100 dilution; Zymed Laboratories) for 1 h at 37°C was followed by incubation with FITC-conjugated goat anti-mouse Abs (1/100 dilution; Jackson ImmunoResearch Laboratories) for 30 min at room temperature. Both Abs were diluted in 1% BSA/PBS to limit aspecific fixation. Cells were washed with PBS and were mounted using a Vectashield reagent to help protect the fluorescence. Cells were visualized using a Zeiss Axiovert microscope equipped for fluorescence and, in most experiments, using the MRC-1024 confocal scanning laser imaging system (Bio-Rad). To evaluate ICAM-1 and VCAM-1 clustering, the extent of specific fluorescence (above a defined threshold) was quantified using image analysis software. For the colabeling of ICAM-1 and caveolin-1, 0.3% Triton X-100 was added to each solution to permeabilize cells. Rabbit anti-caveolin-1 Abs (1/50 dilution; BD Pharmingen) were detected with tetramethylrhodamine isothiocyanate anti-rabbit polyclonal Abs (1/300 dilution; Jackson ImmunoResearch Laboratories). For actin stress fibers visualization, HMVEC cultured on LabTek chambers were fixed with 4% paraformaldehyde for 10 min. Cells were then permeabilized with 0.3% Triton X-100 in PBS and incubated for 1 h with 2 μg/ml FITC-phalloidin (Sigma-Aldrich).

Immunoblotting and NO determination

Immunoblotting was performed on total cell extracts as previously described (14, 15). Both caveolin-1 and eNOS Abs were from BD Pharmingen. The amounts of NO derivatives (NOx) accumulated in the cell-bathing medium for a fixed period of 8 h were evaluated using a colorimetric assay (Roche Diagnostic Systems).

Real-time quantitative PCR

HUVEC preincubated with VEGF (100 ng/ml) for a short (30 min) or long (16 h) period were stimulated with TNF-α (40 U/ml) for 90 min. Total RNA was extracted using silica gel membranes (Qiagen), and cDNA was synthesized using random hexamers and SuperScript Reverse Transcriptase (Invitrogen Life Technologies). Real-time quantitative PCR analyses were performed in triplicate using SYBR Green PCR Master Mix (Applied Biosystems) and the following specific primers: human (h) ICAM-1 sense, 5′-GCCAGGAGACACTGCAGACA-3′; hICAM-1 antisense, 5′-TGGCT TCGTCAGAATCACvGTT-3′; hVCAM-1 sense, 5′-TTTGGGAACGAA CACTCTTACC-3′; hVCAM-1 antisense, 5′-CTTGACTGTGATCGGCT TCC-3′; hRPL19 sense, 5′-CAAGCGGATTCTCATGGAACA-3′; and hRPL19 antisense, 5′-TGGTCAGCCAGGAGCTTCTT-3′. PCR fluorescence data were obtained and analyzed with the ABI PRISM 5700 system instrument (Applied Biosystems). Ct (number of cycles needed to generate a fluorescent signal above a predefined threshold) was determined for each sample, and the relative mRNA expression, expressed as fold variation vs the TNF-α condition, was calculated using the $2^{-\Delta\Delta Ct}$ formula after normalization to RPL19 (ΔCt) and determination of the difference in Ct ($\Delta\Delta$Ct) between the various conditions tested.

Statistics

Data are presented for convenience as mean ± SE. Statistical analyses were made using one sample *t* test or one-way ANOVA with a Dunnett test, where appropriate.

Results

VEGF reduces the adhesion of immune cells on activated EC independently of changes in the expression of adhesion molecules

We first compared the short- and long-term effects of VEGF on the adhesion of immune cells on TNF-α-activated EC. Fig. 1*A* shows that both 30-min and 16-h preincubations of EC with 100 ng/ml VEGF prevented the TNF-α-triggered adhesion of immune cells. These observations were obtained in two different models combining either HUVEC and Jurkat T cells (Fig. 1*A*) or HMVEC and freshly isolated human $CD8^+$ T cells (Fig. 1*B*). We further documented that Abs directed against ICAM-1 and VCAM-1 could block 73 ± 6% and 68 ± 4%, respectively, of the attachment of immune cells to TNF-α-treated EC (Fig. 1*C*), proving the direct involvement of these adhesion molecules in our experimental setup. By contrast, Abs directed against selectins only slightly influence the $CD8^+$ T cell adhesion (Fig. 1*C*).

We then used real-time PCR and flow cytometry analyses to determine whether changes in the expression of adhesion molecules accounted for the observed reduction in adhesion. The $\Delta\Delta$Ct analyses (see *Materials and Methods*) revealed that the TNF-α exposure led to a dramatic increase in the mRNA expression of the two adhesion molecules examined, namely, ICAM-1 and VCAM-1 (Fig. 2*A*). When EC were preincubated with VEGF, a lesser induction of the mRNA expression of both adhesion molecules was observed (see Fig. 2*A*). Flow cytometry analyses revealed that for the 16-h preincubation with VEGF, but not the 30-min VEGF exposure, the observed changes in mRNA expression did translate into alteration in the expression of adhesion proteins (Fig. 2*B*). Yet, the 16-h VEGF-dependent decrease in expression (e.g., mean fluorescence intensity) of ICAM-1 and VCAM-1 amounted to only 17 ± 9% and 10 ± 4%, respectively, whereas in

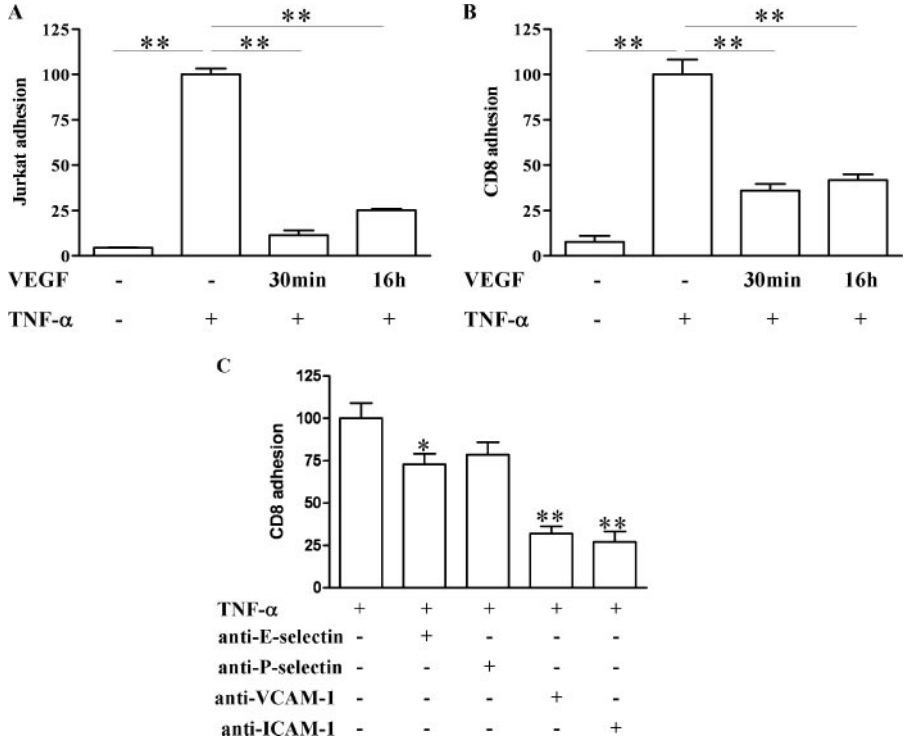

FIGURE 1. TNF-α-induced adhesion of lymphocytes on EC is prevented by VEGF and largely dependent on ICAM-1 and VCAM-1. Confluent HUVEC (*A*) and HMVEC (*B*) monolayers were treated (or not) with VEGF (100 ng/ml) for the indicated period of time (30 min or 16 h) before stimulation with TNF-α (40 U/ml, 4 h). Adhesion of Jurkat cells or $CD8^+$ T cells, respectively, was then evaluated as described in *Materials and Methods*. In some experiments, blocking Abs directed against the indicated adhesion molecules were used (*C*). The results (mean $\pm$ SE) are derived from the immune cell counting within three to four microscopic fields in three separate experiments and are expressed as percentage of the adhesion in the presence of TNF-α (fixed at 100%); *, $p < 0.05$ and **, $p < 0.01$.

the same experiment, the same long-term VEGF stimulus reduced the adhesion by >75% (see Fig. 1*A*).

VEGF-dependent alteration in TNF-α-induced adhesion is regulated by caveolin-1

To understand the reasons of the VEGF effects on lymphocyte adhesion (independently of alterations in the expression of adhesion molecules), we examined how VEGF exposure did influence the distribution of ICAM-1 and VCAM-1 in activated EC. Fig. 3*A* shows that treatment of EC with TNF-α led to a punctate ICAM-1 staining in a large proportion of cells (Fig. 3*A*, *left panels*). Of note, ICAM-1 labeling of unstimulated EC did not reveal any staining over background (data not shown). Interestingly, following a short (30 min) pre-exposure to VEGF,

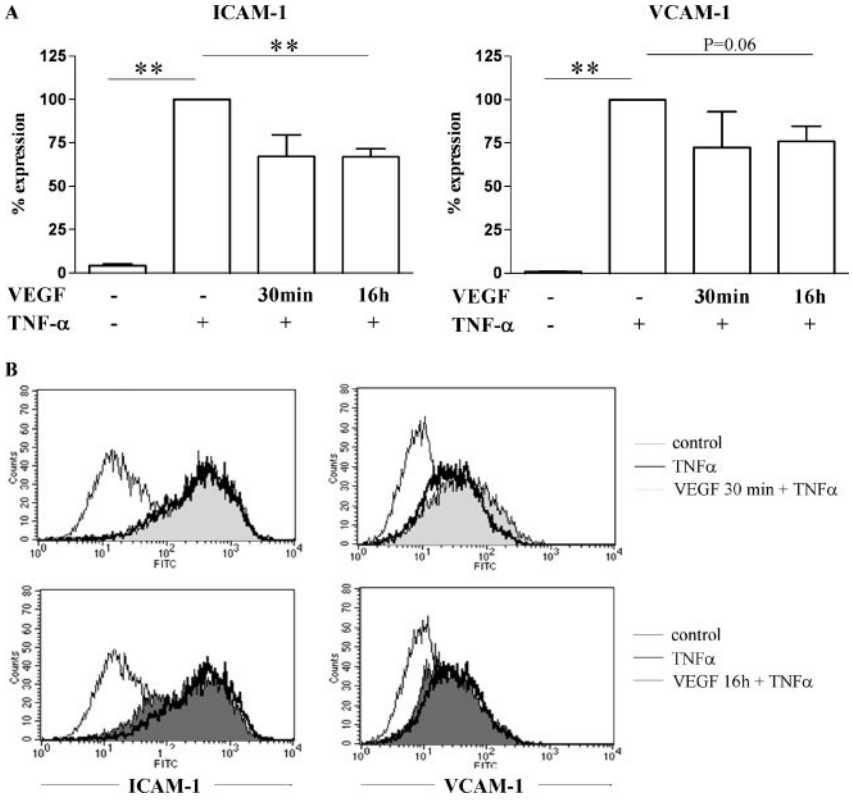

FIGURE 2. VEGF treatment marginally influences the induction of ICAM-1 and VCAM-1 expression by TNF-α. Confluent HUVEC monolayers were (or were not) treated with VEGF (100 ng/ml) for the indicated period of time (30 min or 16 h) before stimulation with TNF-α (40 U/ml). Expression of ICAM-1 (*left*) and VCAM-1 (*right*) was then determined at the mRNA level using RT-PCR (*A*) and at the protein level using flow cytometry (*B*). The results in *A* (mean $\pm$ SE) are expressed as a percentage of the mRNA transcript expression level in the presence of TNF-α (fixed at 100%); **, $p < 0.01$, $n = 3$. The data presented in *B* (surface expression of cell adhesion molecule) are representative of three different experiments.

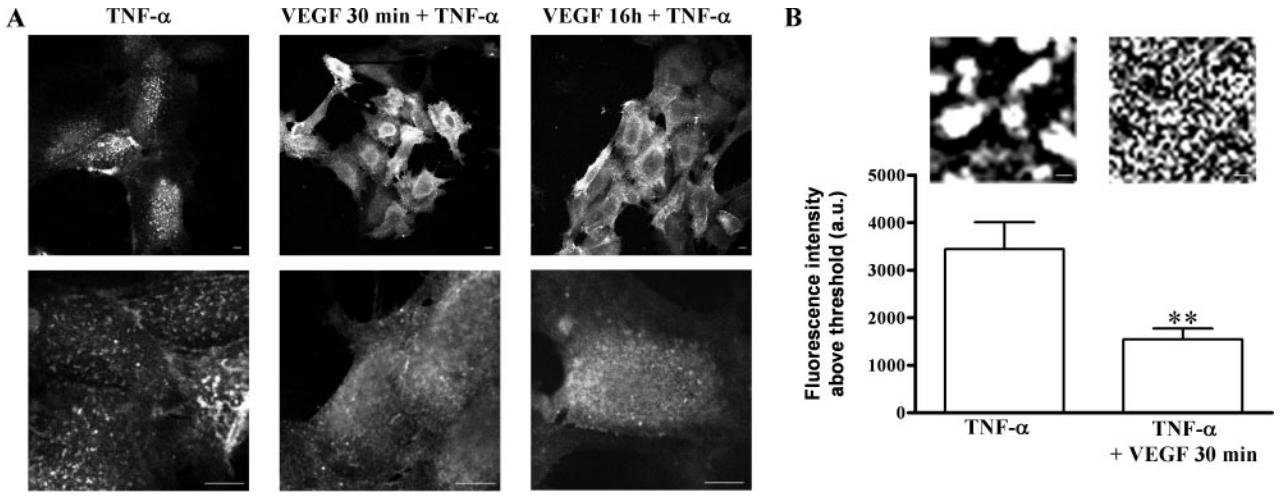

FIGURE 3. VEGF treatment alters the TNF-α-induced ICAM-1 clustering in EC. HUVEC (cultured on LabTek) were treated (or not) with VEGF (100 ng/ml) for the indicated period of time (30 min or 16 h) before stimulation with TNF-α (40 U/ml, 4 h). *A*, Representative micrographs (of five independent experiments) of ICAM-1 immunodetection using confocal microscopy (scale bar, 10 μm). *B*, Quantification of the effects of VEGF 30 min on the ICAM-1 clustering. Representative high magnification confocal images (scale bar, 1 μm) and quantification from 10 to 20 fields per experiment are presented (**, $p < 0.01$, $n = 3$).

ICAM-1 clustering in response to TNF-α stimulation was barely detectable; the staining appeared more diffuse and consistently presented a perinuclear localization (Fig. 3*A*, *middle panels*). A similar pattern of ICAM-1 distribution was observed following longer (16 h) VEGF treatment (Fig. 3*A*, *right panels*). Higher magnification of confocal microscopy images confirmed the deficit in the formation of large ICAM-1 clusters when cells were pre-exposed to VEGF (see Fig. 3*B*); quantification was performed by comparing the number of discrete spots that reached a defined threshold of fluorescence intensity (Fig. 3*B*). Similar experiments were designed to study the potential effect of VEGF on VCAM-1 clustering; a trend toward an ~25% decrease in VCAM-1 clustering was observed in the presence of VEGF using the same methodological approach (data not shown). The low signal-to-noise ratio of the VCAM-1 immunofluorescent signal led us to focus on the sole ICAM-1 clustering in the rest of our study.

Detergent-insoluble membranes (such as rafts and caveolae) (16–18) and, more recently, transmigratory caveolin-1-rich structures (11, 12), were reported to participate in leukocyte adhesion and extravasation (see Introduction). We, therefore, chose to study the potential role of caveolin-1, the structural protein of caveolae, in controlling the inhibitory effects of VEGF on lymphocyte adhesion. We transfected HMVEC with

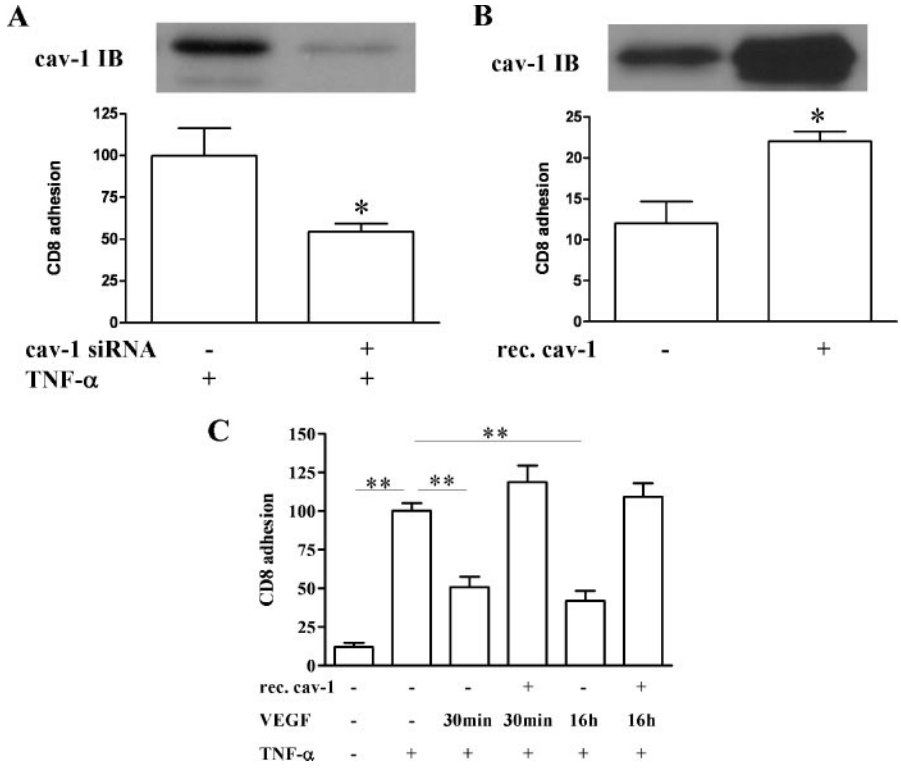

FIGURE 4. Caveolin-1 (cav-1) abundance regulates the extent of lymphocyte adhesion on EC. Confluent HMVEC monolayers were (or were not) transfected with caveolin-1 siRNA (*A*) or caveolin-1 cDNA (*B* and *C*) 24 h before evaluating $CD8^+$ T cell adhesion. Immunoblots (IB) show the consecutive down-regulation and overexpression of caveolin-1, respectively. When indicated, cells were treated with TNF-α (40 U/ml, 4 h) following (or not following) preincubation with VEGF (100 ng/ml) for the indicated period of time (30 min or 16 h). The results (mean ± SE) are derived from the lymphocyte counting within three to four microscopic fields in three separate experiments and are expressed as a percentage of the adhesion in the presence of TNF-α (fixed at 100%); *, $p < 0.05$ and **, $p < 0.01$.

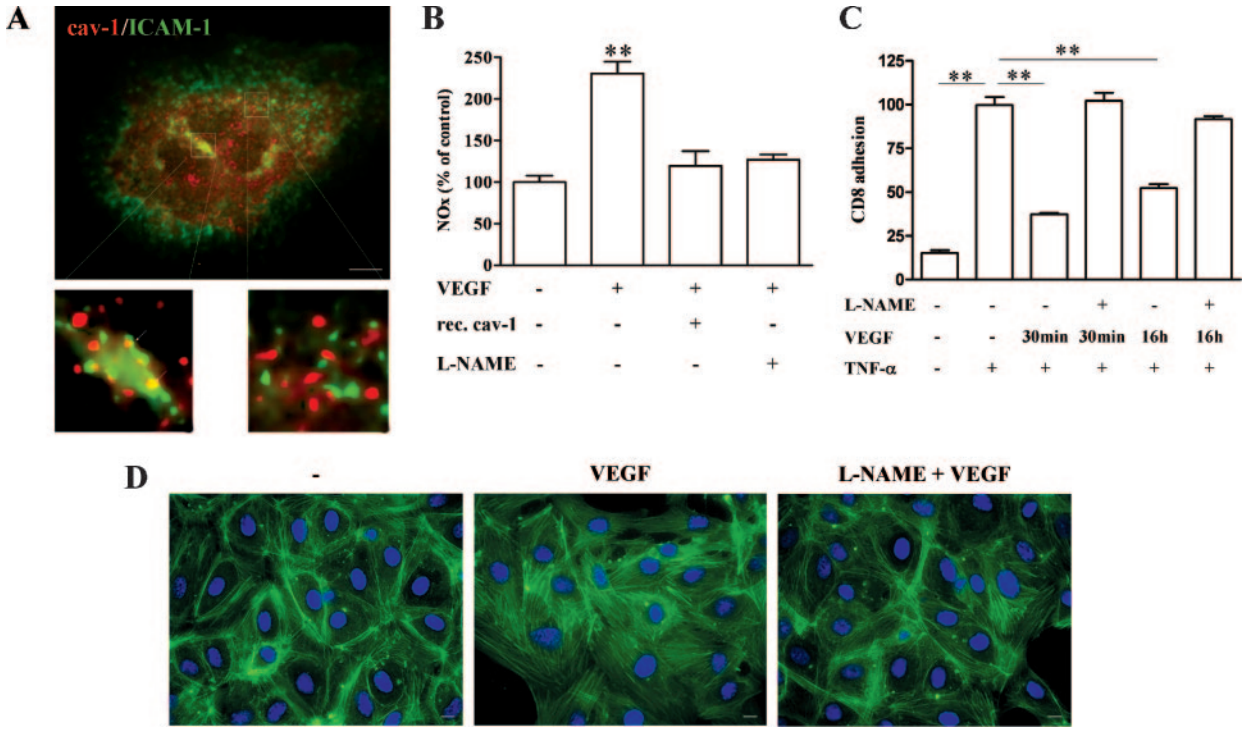

FIGURE 5. NO mediates the VEGF-dependent modulation of lymphocyte adhesion in a caveolin-dependent manner. *A*, Representative micrograph of the TNF-α-induced distribution of caveolin-1 (cav-1, red) and ICAM-1 (green) in HMVEC (cultured on coverslips), as revealed by immunodetection after cell permeabilization; higher magnification reveals some extent of perinuclear costaining, but a complete lack of colocalization in other cell areas. Scale bar, 10 μm. *B*, The effect of caveolin-1 overexpression in EC (same as in Fig. 4*B*) on VEGF-stimulated eNOS activity was compared with the effects of the NOS inhibitor L-NAME. The results (mean $\pm$ SE) are expressed as percentage of NOx accumulated in the extracellular medium under basal conditions; **, $p < 0.01$, $n = 3$–4. Also presented are the effects of L-NAME pretreatment (5 mM) on the VEGF-mediated modulation of both the $CD8^+$ T cell adhesion (*C*) and the cytoskeleton reorganization using FITC-phalloidin labeling of actin fibers; bar scale, 10 μm (*D*). *C*, Results (mean $\pm$ SE) are derived from the lymphocyte counting within three to four microscopic fields in three separate experiments and are expressed as percentage of the adhesion in the presence of TNF-α (fixed at 100%); **, $p < 0.01$.

either a caveolin-1 siRNA or a caveolin-1-encoding plasmid and evaluated the ability of $CD8^+$ T cells to adhere to the transduced cells. As presented in Fig. 4*A*, the extent of the siRNA-mediated down-regulation of caveolin-1 amounted to ~90% and was associated with a 45 $\pm$ 5% inhibition of the TNF-α-induced adhesion. Similar data were obtained with a second caveolin-1 siRNA, but not with a siRNA with one nucleotide mismatched, which was unable to silence caveolin-1 expression (data not shown). By contrast, overexpression of caveolin-1 in HMVEC enhanced the basal adhesion of $CD8^+$ T cells (see Fig. 4*B*); changes in ICAM-1/VCAM-1 clustering were, however, not detectable in these basal conditions considering the low absolute levels of the adhesion molecules in the absence of TNF-α stimulation. We then tested the ability of caveolin-1 transfection to correct the inhibitory effects of VEGF on TNF-α-stimulated adhesion. Overexpression of caveolin-1 restored normal TNF-α-induced adhesion levels in the two conditions tested (e.g., after short- and long-term VEGF preincubations, Fig. 4*C*). Furthermore, a net increase in ICAM-1 clustering was concomitantly authenticated in the presence of recombinant caveolin-1 expression (+61 $\pm$ 27% vs TNF plus VEGF conditions; $p < 0.05$).

NO mediates the VEGF-induced anergy of EC vs immune cells

Because of the apparent key role of caveolin-1 in regulating $CD8^+$ T cell adhesion, we next examined the possible clustering of ICAM-1 with native caveolin-1 after TNF-α stimulation. However, we failed to detect a major colocalization of endogenous caveolin-1 and ICAM-1 in our experimental setup (Fig. 5*A*). We then postulated that caveolin-1 played a role in adhesion through downstream effectors instead of (or in addition to) regulating the compartmentation of proteins involved in leukocyte transmigration. The known inhibitory interaction between caveolin-1 and eNOS (19), and the well-characterized anti-inflammatory properties of NO (20), led us to hypothesize that VEGF could alter the T cell adhesion in a caveolin/eNOS axis-dependent manner.

Accordingly, we found that caveolin-1 overexpression reduced NOx production to the same extent as the NO synthase (NOS) inhibitor L-NAME (Fig. 5*B*). Also, L-NAME treatment appeared to prevent the reduction in adhesion observed following VEGF stimulation (Fig. 5*C*). To further establish in our experimental setup, the link between NO and the VEGF-induced cytoskeletal alterations (known to govern adhesion molecule clustering), we examined the effects of L-NAME on the polymerization of actin fibers. Using the FITC-phalloidin-labeling technique, we validated that the NOS inhibitor significantly prevented the actin fiber reorganization observed upon VEGF stimulation (Fig. 5*D*).

Finally, to support the role of NO in this process, we examined the effect of a NO donor in our experimental adhesion model. We found that DETA-NO inhibited both the TNF-α-induced adhesion (Fig. 6*A*) and ICAM-1 clustering (Fig. 6*B*).

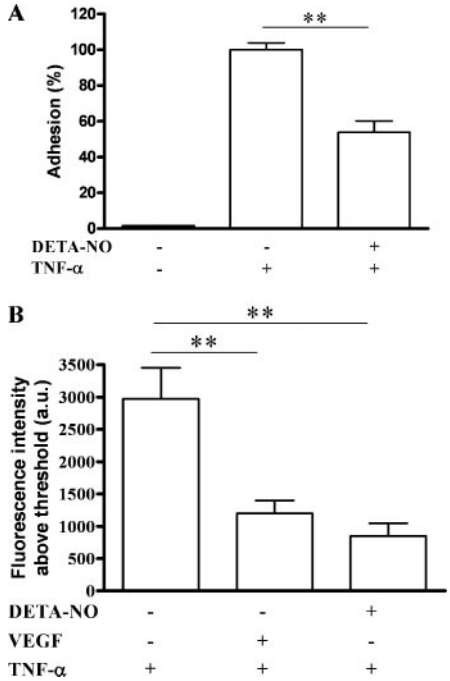

FIGURE 6. NO donor inhibits lymphocyte adhesion and ICAM-1 clustering. Confluent HUVEC monolayers were (or were not) treated with DETA-NO (100 μM) 15 min before TNF-α exposure (40 U/ml, 4 h). *A*, Adhesion of Jurkat T cells was then evaluated. The results (mean $\pm$ SE) are derived from the immune cell counting within three to four microscopic fields and are expressed as percentage of the adhesion in the presence of TNF-α (fixed at 100%). *B*, Quantification (mean $\pm$ SEM) of the ICAM-1 clustering after the DETA-NO exposure; 10–20 high-magnification confocal micrographs were considered per condition and quantification was performed as described in Fig. 3*B*. **, $p < 0.01$.

Discussion

Tumor angiogenesis is known to be associated with a defect in lymphocyte recruitment via a decrease in the expression of adhesion molecules, and particularly ICAM-1 (4, 6, 9). The recently identified roles of caveolae in both the regulation of angiogenesis (13, 14, 19, 21) and the transmigration of lymphocytes (11, 12), however, suggest other mechanisms to account for the anergy of EC lining tumor blood vessels. In this study, we have now documented that 1) the proangiogenic growth factor VEGF can reduce the adhesive capacity of immune cells to activated EC independent of changes in the abundance of adhesion molecules through the alteration of the adhesion molecule clustering process and 2) the role of caveolin-1 in the lymphocyte recruitment process is not restricted to its structural participation to the transcytotic channel, but also involves the modulation of NO-dependent signaling in the initial adhesion process.

The effects of VEGF on the immune cell recruitment process is complex, with different studies reporting the stimulation or the inhibition of the adhesion to EC or both (5, 6, 22–24). However, if one considers conditions where EC are activated (e.g., pre-exposed to proinflammatory cytokines), the consensual view is that angiogenic cytokines impair immune cell adhesion. For instance, Griffioen et al. (5) documented a reduced expression of adhesion molecules after 3-day treatments of TNF-α-stimulated HUVEC with basic fibroblast growth factor or VEGF. Similarly, we observed a reduced induction of ICAM-1 and VCAM-1 mRNA transcripts by TNF-α in the presence of VEGF. Such effects were detectable as early as 2 h after VEGF addition, indicating the rapid modification of the gene expression pattern associated to this angiogenic growth factor. However, after a 16-h VEGF treatment, the protein expression levels of VCAM-1 and ICAM-1 were still barely altered, whereas a dramatic inhibition of $CD8^+$ lymphocytes adhesion was observed. Our confocal analysis revealed that this inhibitory effect on adhesion (also detectable after short VEGF treatment) was associated to a perturbation of the spatial organization of ICAM-1 (and, to a lesser extent, of VCAM-1) at the endothelial surface. Clustering of ICAM-1 was indeed prevented by VEGF, probably through an effect on NO-dependent actin fiber reorganization (see Fig. 5). It is worth noting that a similar scenario was recently reported for atorvastatin (25) that decreased adhesion of monocytes on TNF-α-activated HUVECs through an alteration of the clustering of adhesion molecules despite an increased expression of surface expression.

It is well established that activated adhesion molecules are translocated to rafts or cytoskeletal-associated, detergent-insoluble membranes (16–18) in response to proinflammatory cytokines. The cardinal importance of this early process was recently acknowledged by the identification of a subclass of rafts, namely, caveolae, as critical actors in the structure of the transmigratory channels (11, 12). In this study, we showed that caveolin-1, the structural protein of caveolae, directly influenced the adhesion process. Yet, although the caveolin-1 overexpression was found to restore ICAM-1 clustering and immune cell adhesion, we did not observe a clear colocalization of ICAM-1 and caveolin-1 in our experiments. Although subtle changes in the compartmentation of adhesion molecules into caveolae structures cannot be excluded, our data identified another reason for the exquisite relationship between caveolin-1 abundance and adhesion. We provide evidence that the key modulator of immune cell adhesion is NO, the production of which is stimulated in the presence of VEGF. Caveolin-1 acts, in this study as previously documented (15, 26), as a competitive inhibitor of eNOS. Hence, we showed that an artificial increase in caveolin-1 expression could prevent the NO production observed in response to VEGF, and thereby restored a normal adhesion of lymphocytes to TNF-α-activated EC. Inversely, a NO donor was shown to mimic the potentiation of eNOS activation by caveolin-1 down-regulation and to consecutively reduce immune cell adhesion.

Interestingly, changes in caveolin-1 abundance are reported in certain pathological conditions, which reinforces the paradigm that we have established in this study by using genetic means of altering caveolin-1 expression (i.e., caveolin-1 siRNA or encoding plasmid). For instance, caveolin-1 expression was found to be down-regulated in cultured EC exposed to angiogenic growth factors (27) and in vivo in the tumor microvasculature (vs vessels from healthy tissues) (28). In our laboratory, we also recently documented that angiogenesis is stimulated in tumors established in caveolin-deficient animals and that hypoxia, as encountered in tumors, rapidly leads to a reduction in caveolin-1 expression in EC (data not shown). The very high rate of tumor growth in the xenograft model (i.e., B16 melanoma) used in caveolin-deficient mice, however, precluded any dissection of the immune cell recruitment process and/or of a direct effect on tumor growth. Yet, these data reinforce the paradigm of the NO-mediated anergy of angiogenic EC induced by caveolin-1 down-regulation and emphasize that caveolin-1 could be a possible target to reverse such phenomenon.

We, and others, have previously documented that increasing the inhibitory effect of caveolin-1 on tumor angiogenesis by in vivo lipofection of caveolin-1 cDNA (15) or i.p. administration of caveolin-1-derived peptides (21) was an achievable therapeutic goal. Further studies are needed to explore whether such caveolin-targeting approaches or, more generally, antiangiogenic strategies may increase the clinical efficacy of cancer immunotherapy.

Acknowledgments

We thank M. Teke (Institut Paul Lambin) for excellent technical assistance, A. Tonon (Ludwig Institute, Université Catholique de Louvain Medical School) for advice on FACS studies and P. Courtoy (Universite Catholique de Louvain Medical School) for access to confocal microscope facilities.

Disclosures

The authors have no financial conflict of interest.

References

1. Greten, T. F., and E. M. Jaffee. 1999. Cancer vaccines. *J. Clin. Oncol.* 17: 1047–1060.
2. Li, Q., and A. E. Chang. 1999. Adoptive T-cell immunotherapy of cancer. *Cytokines Cell Mol. Ther.* 5: 105–117.
3. Yu, Z., and N. P. Restifo. 2002. Cancer vaccines: progress reveals new complexities. *J. Clin. Invest.* 110: 289–294.
4. Wu, N. Z., B. Klitzman, R. Dodge, and M. W. Dewhirst. 1992. Diminished leukocyte-endothelium interaction in tumor microvessels. *Cancer Res.* 52: 4265–4268.
5. Griffioen, A. W., C. A. Damen, G. H. Blijham, and G. Groenewegen. 1996. Tumor angiogenesis is accompanied by a decreased inflammatory response of tumor-associated endothelium. *Blood* 88: 667–673.
6. Griffioen, A. W., C. A. Damen, S. Martinotti, G. H. Blijham, and G. Groenewegen. 1996. Endothelial intercellular adhesion molecule-1 expression is suppressed in human malignancies: the role of angiogenic factors. *Cancer Res.* 56: 1111–1117.
7. Jain, R. K., G. C. Koenig, M. Dellian, D. Fukumura, L. L. Munn, and R. J. Melder. 1996. Leukocyte-endothelial adhesion and angiogenesis in tumors. *Cancer Metastasis Rev.* 15: 195–204.
8. Kitayama, J., H. Nagawa, H. Yasuhara, N. Tsuno, W. Kimura, Y. Shibata, and T. Muto. 1994. Suppressive effect of basic fibroblast growth factor on transendothelial emigration of $CD4^+$ T-lymphocyte. *Cancer Res.* 54: 4729–4733.
9. Melder, R. J., G. C. Koenig, B. P. Witwer, N. Safabakhsh, L. L. Munn, and R. K. Jain. 1996. During angiogenesis, vascular endothelial growth factor and basic fibroblast growth factor regulate natural killer cell adhesion to tumor endothelium. *Nat. Med.* 2: 992–997.
10. Liu, D., H. Jia, D. I. Holmes, A. Stannard, and I. Zachary. 2003. Vascular endothelial growth factor-regulated gene expression in endothelial cells: KDR-mediated induction of Egr3 and the related nuclear receptors Nur77, Nurr1, and Nor1. *Arterioscler. Thromb. Vasc. Biol.* 23: 2002–2007.
11. Carman, C. V., and T. A. Springer. 2004. A transmigratory cup in leukocyte diapedesis both through individual vascular endothelial cells and between them. *J. Cell Biol.* 167: 377–388.
12. Millan, J., L. Hewlett, M. Glyn, D. Toomre, P. Clark, and A. J. Ridley. 2006. Lymphocyte transcellular migration occurs through recruitment of endothelial ICAM-1 to caveola- and F-actin-rich domains. *Nat. Cell Biol.* 8: 113–123.
13. Labrecque, L., I. Royal, D. S. Surprenant, C. Patterson, D. Gingras, and R. Beliveau. 2003. Regulation of vascular endothelial growth factor receptor-2 activity by caveolin-1 and plasma membrane cholesterol. *Mol. Biol. Cell* 14: 334–347.
14. Sonveaux, P., P. Martinive, J. DeWever, Z. Batova, G. Daneau, M. Pelat, P. Ghisdal, V. Gregoire, C. Dessy, J. L. Balligand, and O. Feron. 2004. Caveolin-1 expression is critical for vascular endothelial growth factor-induced ischemic hindlimb collateralization and nitric oxide-mediated angiogenesis. *Circ. Res.* 95: 154–161.
15. Brouet, A., J. DeWever, P. Martinive, X. Havaux, C. Bouzin, P. Sonveaux, and O. Feron. 2005. Antitumor effects of in vivo caveolin gene delivery are associated with the inhibition of the proangiogenic and vasodilatory effects of nitric oxide. *FASEB J.* 19: 602–604.
16. Amos, C., I. A. Romero, C. Schultze, J. Rousell, J. D. Pearson, J. Greenwood, and P. Adamson. 2001. Cross-linking of brain endothelial intercellular adhesion molecule (ICAM)-1 induces association of ICAM-1 with detergent-insoluble cytoskeletal fraction. *Arterioscler. Thromb. Vasc. Biol.* 21: 810–816.
17. Tilghman, R. W., and R. L. Hoover. 2002. E-selectin and ICAM-1 are incorporated into detergent-insoluble membrane domains following clustering in endothelial cells. *FEBS Lett.* 525: 83–87.
18. Yoshida, M., W. F. Westlin, N. Wang, D. E. Ingber, A. Rosenzweig, N. Resnick, and M. A. Gimbrone, Jr. 1996. Leukocyte adhesion to vascular endothelium induces E-selectin linkage to the actin cytoskeleton. *J. Cell Biol.* 133: 445–455.
19. Sbaa, E., F. Frerart, and O. Feron. 2005. The double regulation of endothelial nitric oxide synthase by caveolae and caveolin: a paradox solved through the study of angiogenesis. *Trends Cardiovasc. Med.* 15: 157–162.
20. Ahluwalia, A., P. Foster, R. S. Scotland, P. G. McLean, A. Mathur, M. Perretti, S. Moncada, and A. J. Hobbs. 2004. Antiinflammatory activity of soluble guanylate cyclase: cGMP-dependent down-regulation of P-selectin expression and leukocyte recruitment. *Proc. Natl. Acad. Sci. USA* 101: 1386–1391.
21. Gratton, J. P., M. I. Lin, J. Yu, E. D. Weiss, Z. L. Jiang, T. A. Fairchild, Y. Iwakiri, R. Groszmann, K. P. Claffey, Y. C. Cheng, and W. C. Sessa. 2003. Selective inhibition of tumor microvascular permeability by cavtratin blocks tumor progression in mice. *Cancer Cells* 4: 31–39.
22. Min, J. K., Y. M. Lee, J. H. Kim, Y. M. Kim, S. W. Kim, S. Y. Lee, Y. S. Gho, G. T. Oh, and Y. G. Kwon. 2005. Hepatocyte growth factor suppresses vascular endothelial growth factor-induced expression of endothelial ICAM-1 and VCAM-1 by inhibiting the nuclear factor-κB pathway. *Circ. Res.* 96: 300–307.
23. Detmar, M., L. F. Brown, M. P. Schon, B. M. Elicker, P. Velasco, L. Richard, D. Fukumura, W. Monsky, K. P. Claffey, and R. K. Jain. 1998. Increased microvascular density and enhanced leukocyte rolling and adhesion in the skin of VEGF transgenic mice. *J. Invest. Dermatol.* 111: 1–6.
24. Dirkx, A. E., M. G. Oude Egbrink, M. J. Kuijpers, S. T. van der Niet, V. V. Heijnen, J. C. Bouma-ter Steege, J. Wagstaff, and A. W. Griffioen. 2003. Tumor angiogenesis modulates leukocyte-vessel wall interactions in vivo by reducing endothelial adhesion molecule expression. *Cancer Res.* 63: 2322–2329.
25. Bernot, D., A. M. Benoliel, F. Peiretti, S. Lopez, B. Bonardo, P. Bongrand, I. Juhan-Vague, and G. Nalbone. 2003. Effect of atorvastatin on adhesive phenotype of human endothelial cells activated by tumor necrosis factor α. *J. Cardiovasc. Pharmacol.* 41: 316–324.
26. Ikeda, S., M. Ushio-Fukai, L. Zuo, T. Tojo, S. Dikalov, N. A. Patrushev, and R. W. Alexander. 2005. Novel role of ARF6 in vascular endothelial growth factor-induced signaling and angiogenesis. *Circ. Res.* 96: 467–475.
27. Liu, J., B. Razani, S. Tang, B. I. Terman, J. A. Ware, and M. P. Lisanti. 1999. Angiogenesis activators and inhibitors differentially regulate caveolin-1 expression and caveolae formation in vascular endothelial cells: angiogenesis inhibitors block vascular endothelial growth factor-induced down-regulation of caveolin-1. *J. Biol. Chem.* 274: 15781–15785.
28. Regina, A., J. Jodoin, P. Khoueir, Y. Rolland, F. Berthelet, R. Moumdjian, L. Fenart, R. Cecchelli, M. Demeule, and R. Beliveau. 2004. Down-regulation of caveolin-1 in glioma vasculature: modulation by radiotherapy. *J. Neurosci. Res.* 75: 291–299.